

MINERALOGICAL STUDY AND PROPERTIES OF MAGNESIA REFRACTORIES DERIVED FROM EVIAN MAGNESITE

Lampropoulou P.¹ and Katagas C.¹,

¹ Section of Earth Materials, Department of Geology, University of Patras, 26500 Patras,
P.Lampropoulou@upatras.gr, C.Katagas@upatras.gr

ABSTRACT

In order for the Greek magnesia industry to retain a high position in the world market, the basic refractories derived from Greek magnesite must remain at the forefront of the international developments.

A mineralogical study of magnesia materials produced from Evian magnesite has been carried out with the aim a) to provide detailed characterization of products and microstructures derived from the firing processes of magnesia raw materials and b) to contribute to the development of new magnesia-spinel refractory materials from natural Greek magnesite.

The magnesite of N. Evia, Greece, is micro-crystalline and has been used for the production of basic refractories because of the very low amounts of impurities such as CaO, SiO₂, FeO(tot), B₂O₃ it contains .

Magnesia materials studied here are:

1) Raw materials. The dead-burned magnesia grains examined are divided into two groups according to the mode of beneficiation of the raw magnesite:

a) Dead burned magnesias produced from natural microcrystalline magnesite (Group A).

b) Dead burned magnesias of high purity produced from natural microcrystalline magnesite (Group B).

The chemical composition of these materials lies essentially in the MgO-CaO-SiO₂ system, since they contain only trace amounts of Fe₂O₃ and Al₂O₃. Their microstructures vary widely in terms of proportions of direct MgO-MgO bonding, amounts and types of phases of the siliceous bonding and size of the periclase crystals. Dead burned magnesias of high purity are better sintered and contain lower amounts of secondary phases compared to magnesias of lower purity.

2) Commercial magnesia bricks derived from dead burned magnesia of high purity and magnesia chromite bricks derived from raw materials of dead burned magnesia of high purity and chromite from Africa.

3) New spinel-based composition and new magnesia-spinel refractory materials which have been synthesized for the needs of this study.

The newly synthesized spinel-based composition (70wt% Al₂O₃-30wt% MgO) shows an increase in the bulk density as well as in the amount of spinel formed compared to available commercial qualities (50%wt Al₂O₃).

4) Using this new spinel-based composition and dead burned magnesia of high purity, two new magnesia-spinel refractory materials containing 10 and 20wt% Al₂O₃ were produced, with the aim to obtain more friendly to the environment magnesia refractories to substitute for the magnesia chromite bricks. The compositions of the magnesia spinel refractories thus produced were expected to show endurance in thermal shocks as well as in the corrosion from slags and friction, in order to have a wide application in steel, cement industry etc .

1 INTRODUCTION

A mineralogical study of magnesia materials produced from Evian magnesite has been carried out with aim a) to provide detailed characterization of the products and microstructures derived from

the firing processes of magnesia raw materials from Mantoudi and b) to contribute to the development of new magnesia-spinel refractory materials from natural Greek magnesite.

2 RESULTS AND DISCUSSION

2.1 Magnesite

The magnesite of N.Evia, Greece is microcrystalline and has been used for the production of basic refractories because of the very low amounts of impurities such as CaO, SiO₂, FeO(tot) and B₂O₃ it contains (Foroglou 1985) (Tab. 1, Fig. 1).

Table 1. Representative composition of bulk magnesite (1 and 2) and typical microanalysis of a magnesite aggregate (3) from N.Evia

	1	2	3
SiO ₂	0.25	0.10	0.00
Al ₂ O ₃	0.03	0.02	0.00
Fe ₂ O ₃	0.02	0.34	0.21
MnO	0.00	0.04	0.00
MgO	45.69	46.79	47.02
CaO	3.37	0.64	0.80
K ₂ O	0.01	0.05	0.00
Cr ₂ O ₃	0.01	0.00	0.00
CO ₂	50.89	52.05	

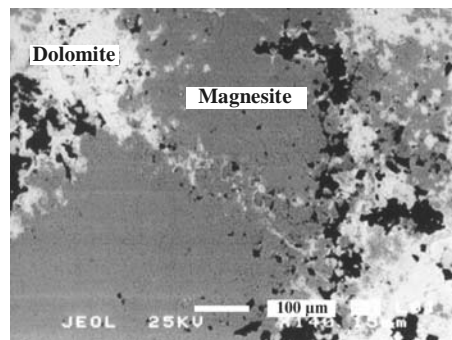


Figure 1. Cryptocrystalline magnesite and dolomite (SEM)

2.2 Dead burned magnesia and fused magnesia

The production of refractory materials is based on the dead burned magnesia, a product containing periclase as a major phase, derived from calcined magnesite. The dead-burned magnesia grains examined here were divided into groups A and B, according to the mode of beneficiation of the raw magnesite. Dead-burned magnesias of group A (E21A, E12E, NE3) were produced from natural microcrystalline magnesite by firing at temperatures in the range of 1850-1900 °C in rotary kilns. Prior to dead burning, magnesite was beneficiated by conventional methods (optical sorting, heavy media, magnetic separation). Magnesias of group B (MSA, MA) were produced from natural microcrystalline magnesite beneficiated by froth flotation, which ensures homogeneity and low silica. The obtained filter cake is calcined to caustic magnesia, which is subsequently briquetted and dead burned in a shaft kiln at temperatures up to 2000 °C.

A fused magnesia (FC) grain of Chinese origin was studied for comparative reasons only. It is produced by melting raw or calcined magnesia in an electric-arc furnace at temperatures of >2750°C. The fused magnesia is superior to dead burned magnesia in terms of strength, abrasion resistance and chemical reactivity but is more expensive than dead-burned magnesias.

The chemical composition of these materials lies essentially in the MgO-CaO-SiO₂ system since they contain only trace amounts of FeO(tot) and Al₂O₃ (Tab. 2). Although their CaO/SiO₂ ratios can be used to approximate their mineralogical compositions, detailed XRD, optical and analytical SEM studies revealed significant deviations from the expected phase assemblages (Tab. 3).

Table 2. Chemical analyses of magnesia grains (ICP)

Sample	SiO ₂	Al ₂ O ₃	Fe ₂ O ₃ **	MnO	MgO	CaO	Na ₂ O	K ₂ O	Cr ₂ O ₃	C/A***
A E21A	1.10	0.03	0.82	0.07	95.61	2.36	0.00	0.00	0.02	2.14
A E12E	4.02	0.21	1.76	0.09	89.55	4.15	0.06	0.06	0.13	1.03
A NE3	7.72	0.18	1.40	na	86.49	4.07	N.A.*	N.A.*	0.14	0.53
B MSA	0.79	0.03	0.48	0.05	96.05	2.56	0.03	0.02	0.00	3.24
B MA	0.71	0.03	0.38	0.04	96.00	2.70	0.02	0.06	0.04	3.80
FC	0.35	0.06	0.27	N.A.*	98.26	1.05	N.A.*	N.A.*	0.01	3.00

*N.A.: not analyzed, **total iron as Fe₂O₃, *** C/A: CaO / Al₂O₃

Table 3. Calc-silicate phases coexisting with periclase, and their modal abundances in the magnesia raw materials

Sample	M ₂ S	CMS	C ₃ MS ₂	C ₂ S	C ₃ S	CaO	Periclase Modal (%)	Calc-silicates Modal (%)
E21A		+++	+++	+ e	+ e	+	93.5	6.5
E12E		+++ e	+++ e	+	+	+	87.0	13.0
NE3	+++ e	+++ e	+	+		+	79.0	21.0
MSA			+	+++	e	++ e	98.5	1.5
MA			+	+++	+ e	++ e	98.3	1.7
FC				+++	e	++ e	99.2	0.8

Bonding phases: +++: abundant; ++: frequent; +: sparse; e: phase expected to be present, M₂S:2MgOSiO₂; CMS:CaOMgOSiO₂; C₃MS₂:3CaOMgO₂SiO₂; C₂S:2CaOSiO₂; C₃S:3CaOSiO₂;

Their microstructures vary widely in terms of the size of the main phase (periclase), the proportions of direct MgO-MgO bonding and the amounts and types of the siliceous bonding phases. The qualities of group B magnesia and Fused Chinese Magnesia contain less secondary phases compared to the qualities E21A, E12E and NE3. The chemical compositions of the later qualities favored the formation of secondary calcium-silicate phases of low melting point, (such as mervinite, monticellite), which reduce the refractoriness of the materials. Figure 2 is a SEM image of a magnesia quality with much higher content of impurities (NE3) than the other studied samples. Figure 3 shows the microstructure of a very pure magnesia sample (MSA). It is evident that, the dead burned magnesia of high purity have the largest size of periclase crystals and very low amounts of calc-silicate bonding phases.

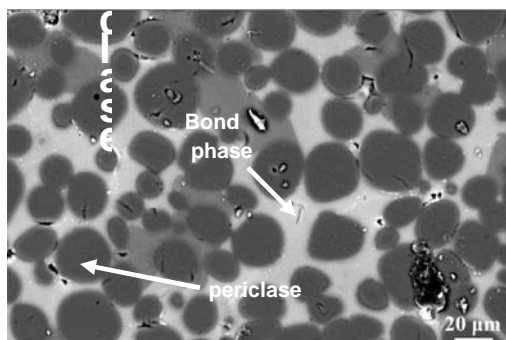


Figure 2. Microstructure of NE3 (SEM)

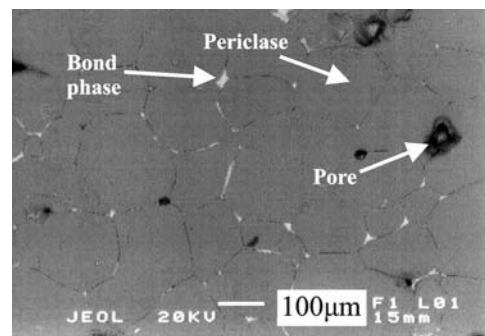


Figure 3. Microstructure of MSA (SEM)

2.3 Commercial bricks

The magnesia brick (Mb) is characterized by the presence of coarse-grained magnesia material connected through fine-grained magnesia (Fig.4) and exhibit good refractoriness. Magnesia chromite bricks (Mcb) are superior to magnesia bricks at high temperatures and behave better in thermal shocks because of their significantly lower thermal factor coefficient and the strength of the MgO-Chromite bond (Fig.5) but they are not friendly to the environment (Goto and Lee, 1995).

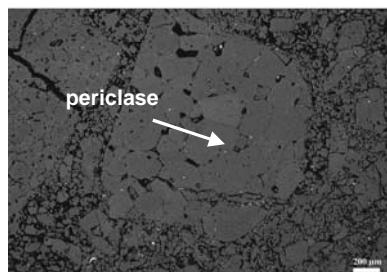


Figure 4. Microstructure of Mb (SEM).

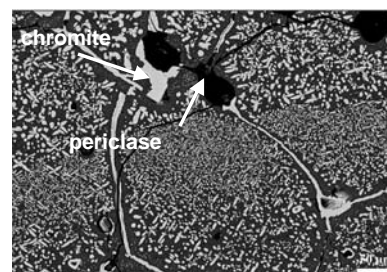


Figure 5. Microstructure of Mcb (SEM).

2.4 New spinel compositions

The new spinel compositions which have been synthesized for the needs of this study were derived from dead burned magnesia of high purity, alumina and chromite as additive (2%). Two qualities, Sp50 and Sp70, which contain approximately 50 and 70wt% alumina respectively have been synthesized and studied. Representative images of their microstructures on polished surfaces are given in Figures 6, 7. An increase in the amount of Al_2O_3 in the spinel based compositions lead to an increase in the bulk density ($3.32, 3.39 \text{ gr/cm}^3$ for Sp50 and Sp70 respectively) as well as in the amount of spinel phase formed. Besides spinel and periclase, low amounts of secondary calcium-aluminate and calcium-silicate phases were traced in the new spinel-based compositions (Tab. 4); not all of them are equilibrium phases. The stabilizing additive Cr_2O_3 enters mainly the lattice of spinel, increases its density and acts as a core for the formation of this mineral. Furthermore, the direct diffusion bondings are stronger than those of the spinel crystals in the spinel compositions without chromite. This microstructure results in an increase of the resistance of spinel against the chemical corrosion from fused metallurgic slags (Peng et. al., 1999). Periclase however, is sometimes hydrated to brucite resulting to cracks of microstructure due to a long exposure of the material to atmosphere (Fig.10).

Table 4. Coexisting phases with spinel and periclase in spinel compositions

Sample	Phases								CaO/SiO ₂
	C ₃ S ₂	C ₂ S	C ₃ S	CaO	C ₃ A	C ₁₂ A ₇	CF ₂	C ₂ AS	
Sp50	+++	+++ e	+ e	++	+ e	+	*	+	2.82
Sp70	++	++ e	++ e	++ e	+++ e	+	*		3.2

Bonding phases: +++: abundant; ++: frequent; +: sparse; e: phase expected to be present C:CaO; S:SiO₂; A:Al₂O₃; F:Fe₂O₃, *: Possible phase

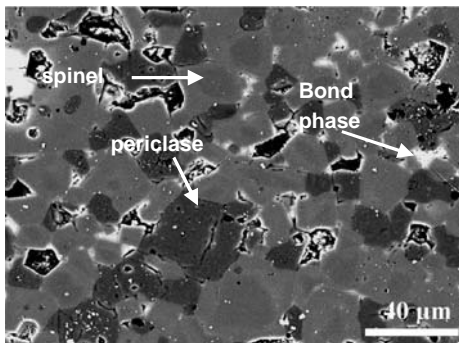


Figure 6. Microstructure of Sp50 (SEM)

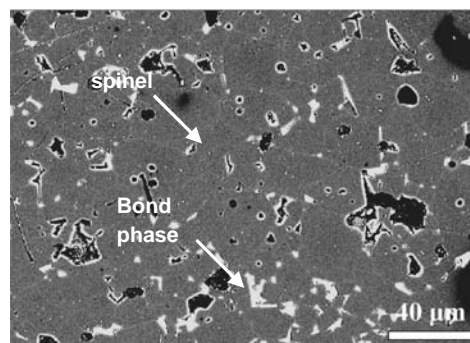


Figure 7. Microstructure of Sp70 (SEM)

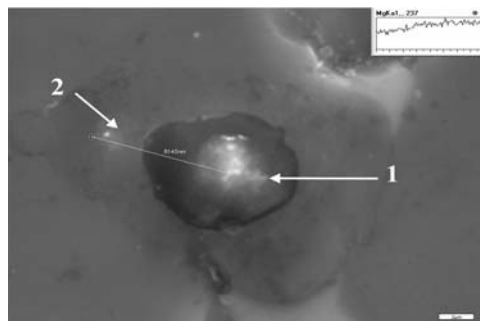


Figure 8. Line scan on a hydrated crystal of periclase

2.5 New magnesia - spinel refractory materials

Using the improved new spinel-based composition Sp70 and dead burned magnesia of high purity MSA, two new magnesia-spinel refractory materials containing 10 and 20 wt% Al_2O_3 (SB70-10 and SB70-20 respectively) were produced, with the aim to obtain more friendly to the environment magnesia spinel refractories to substitute for the magnesia chromite bricks. The compositions of the magnesia spinel refractories thus produced were expected to show endurance in thermal shocks as well as in the corrosion from slags and friction, in order to have a wide application in steel, cement industry etc (Nagasoe et. al., 1991). The secondary calcium-aluminate and calcium silicate phases (Tab. 5) are mainly concentrated in the borders of periclase and spinel grains but are not expected to reduce the refractoriness of the materials because they occur in very low amounts. The exaphosphate additive leads to the formation of the $2\text{CaOSiO}_2\text{-}3\text{CaOP}_2\text{O}_5$ solid solution which stabilizes the phase of C_2S , preventing micro cracks in the microstructure. Estimation of bulk density, cold crushing strength parameter and thermal coefficient factor (Tab. 6), of the new magnesia-spinel refractory materials, revealed that: a) the new refractory materials show high endurance in crushing and in corrosion and b) the refractory material that contains 20 wt % Al_2O_3 exhibits higher endurance in rapid thermal changes than that with 10wt% Al_2O_3 . Characteristic images of their microstructures are given in Figures 9, 10. It is very interesting to note that SEM studies revealed the occurrence of secondary spinel crystals concentrated in the borders of the periclase crystals (Figure 11) thus strengthening their bonding.

Table 5. Secondary phases in magnesia-spinel refractories

Sample	C_2S	C_3S	C_3A	C	$\text{C}_2\text{S-C}_3\text{P}$	C_{12}A_7	C_2AS	CF_2	CaO/SiO_2
SB70-10	+++	++e	+++e	++e	+++	+		*	4.03
SB70-20	+++	++e	+++e	++e	+++	+		*	4.83

Table 6. Bulk density, Cold crushing strength and thermal coefficient factor in magnesia-spinel refractories

Sample	Bulk density (gr/cm^3)	CcS (kp/cm^2)	Thermal coefficient factor ($\times 10^{-6}/\text{K}$)
SB70-10	2.85	351	13.1
SB70-20	2.85	356	12.4

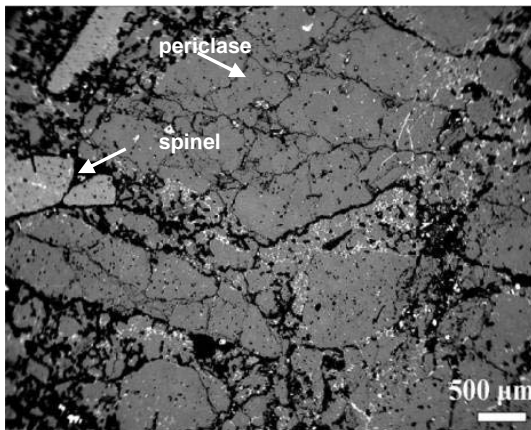


Figure 9. Microstructure of SB70-10 (SEM)

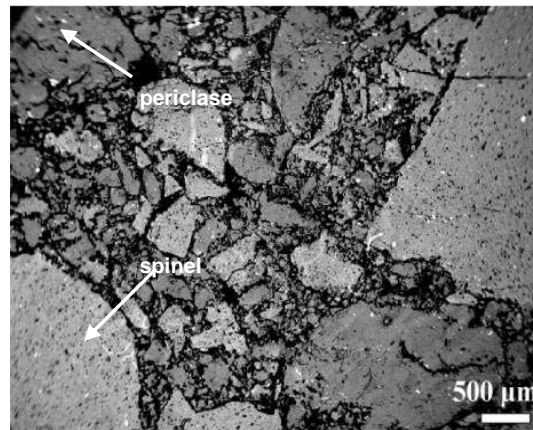


Figure 10. Microstructure of SB70-20 (SEM)

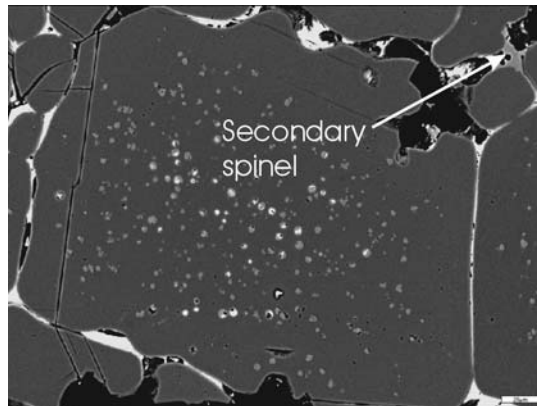


Figure 11. Secondary spinel near the periclase borders (SEM) in magnesia spinel refractory

3 CONCLUSIONS

- 1) The dead burned magnesia of high purity is the most suitable raw material for the production of basic refractories due to the high proportion of direct MgO-MgO bonding and to the low amounts of secondary calcium silicate phases which are formed.
- 2) The new spinel based composition with 70wt% Al_2O_3 (Sp70) which have been synthesized is expected to show good refractoriness due to its high spinel content and its dense microstructure.
- 3) The new, friendly to the environment magnesia-spinel refractories are expected to substitute the magnesia-chromite bricks for high temperature industrial applications, because of their improved properties in rapid thermal changes and in the corrosion from slags.

ACKNOWLEDGEMENTS

The authors wish to thank Mr. V. Kotsopoulos, of the laboratory of Electron Microscopy and Microanalysis, University of Patras, for his help with the Microanalyses and SEM photomicrographs.

REFERENCES

- Foroglou, G., Malissa, H., and Grasserbauer, M., 1980. Microstructural Characterization Study of Magnesia Derived from Natural Microcrystalline Magnesite, *Transactions Journal British Ceramics Society*, 79, 91-97.
- Goto, K., and Lee, W., 1995. The direct bond in Magnesia Chromite and Magnesia Spinel Refractories, *Journal of the American Ceramic Society*, 78, 1753-1760.
- Nagasoe, A., Tsurumoto, S., and Kitamura, A., 1991. Refractory Characteristics of Spinels with various MgO contents, *Taikabutsu Overseas*, 11, 20-28.
- Peng, X., Zhou, K., and Zhang, X., 1999. Effects of Cr_2O_3 on properties of Alumina-Spinel Castable. *China's Refractories*, 8, 6-8.